Article type : MS - Regular Manuscript

Mesophyll conductance does not contribute to greater photosynthetic rate per unit nitrogen in temperate compared to tropical evergreen wet-forest tree leaves

Nur H. A. Bahar[1], Lucy Hayes[1], Andrew P. Scafaro[1], Owen K. Atkin[1] and John R. Evans[2]

[1]ARC Centre of Excellence in Plant Energy Biology, Division of Plant Sciences, Research School of Biology, Australian National University, Canberra, 2601, ACT, Australia; [2]ARC Centre of Excellence for Translational Photosynthesis, Division of Plant Sciences, Research School of Biology, Australian National University, Canberra 2601, ACT, Australia

Author for correspondence:
John R Evans
Tel: +61 2 6125 4492
Email: john.evans@anu.edu.au

Received: *28 August 2017*

Accepted: *23 December 2017*

Summary

- Globally, trees originating from high rainfall tropical regions typically exhibit lower rates of light-saturated net CO_2 assimilation (A) compared to those from high rainfall temperate environments, when measured at a common temperature. One factor that has been suggested to contribute towards lower rates of A is lower mesophyll conductance.
- Using a combination of leaf gas exchange and carbon isotope discrimination measurements, we estimated mesophyll conductance (g_m) of several Australian tropical and temperate wet-forest trees, grown in a common environment. Maximum Rubisco carboxylation capacity, V_{cmax}, was obtained from CO_2 response curves.
- All species fell on a common A–g_m relationship such that the ratios of V_{cmax} : g_m and the drawdown of CO_2 across the mesophyll were both relatively constant. V_{cmax} estimated on the basis of intercellular CO_2 partial pressure, C_i, was equivalent to that estimated using chloroplastic CO_2 partial pressure, C_c, using 'apparent' and 'true' Rubisco Michaelis-Menten constants, respectively.
- Having ruled out g_m as a possible factor in distorting variations in A between these tropical and temperate trees, attention now needs to be focussed on obtaining more detailed information about Rubisco in these species.

Key words: carboxylation capacity, CO_2 drawdown, mesophyll conductance, photosynthetic limitation, temperate, tropical.

Introduction

Tropical and temperate forest ecosystems account for one half of terrestrial net primary productivity and represent a major component of the global carbon stock (Bonan, 2008; Pan *et al.*, 2011; Prentice *et al.*, 2011). While floristically diverse, generalisations have emerged from extensive field measurements of leaves for many tropical and temperate forest species (e.g. Kattge *et al.*, 2011; Atkin *et al.*, 2015). For key leaf attributes, biome-specific mean trait values have been calculated and are routinely used to parameterise ecosystem carbon exchange in Earth system models (Kattge *et al.*, 2009; Verheijen *et al.*, 2013). On average, wet forest tropical trees have slower area-based photosynthetic rates than temperate trees and

less nitrogen (N) per unit leaf area (Kattge *et al.*, 2009; Xiang *et al.*, 2013; Ali *et al.*, 2015). Variations in photosynthetic rates across biomes could be attributed to biochemical factors, such as the amount and allocation of N to photosynthetic machinery (e.g. Rubisco) as well as to diffusional constraints imposed by stomata and the mesophyll (Evans, 1989; Hikosaka *et al.*, 1998; Evans & Loreto, 2000). For example, a greater investment of N in Rubisco might underpin the tendency of temperate trees to exhibit a greater photosynthetic rate and Rubisco carboxylation capacity per unit leaf N than tropical trees (Kattge *et al.*, 2009; Xiang *et al.*, 2013; Ali *et al.*, 2015; Scafaro *et al.*, 2017).

Rubisco carboxylation capacity, V_{cmax}, is derived from gas exchange measurements using the Farquhar, von Caemmerer & Berry (1980) (FvCB) model of C_3 photosynthesis. In order to apply this model, one needs to assume values for three Rubisco kinetic parameters: the Michaelis Menten constants for CO_2 and O_2 (K_c and K_o, respectively) and the CO_2 photocompensation point, Γ_*. Unfortunately, due to the difficulty in determining *in vivo* values for these parameters, one generally assumes values obtained from tobacco (Bernacchi *et al.*, 2001, 2002). Potential differences in Rubisco kinetic parameters among species are ignored (Galmés *et al.*, 2016). A second issue is whether one uses the partial pressure of CO_2 in the intercellular airspaces, C_i, or in the chloroplast, C_c, during the derivation. While C_i is readily obtained from conventional gas exchange measurements, calculating C_c requires additional instruments that measure chlorophyll fluorescence or stable isotope discrimination (Evans *et al.*, 1986; von Caemmerer & Evans, 1991; Harley *et al.*, 1992; Loreto *et al.*, 1992; Pons *et al.*, 2009) which until recently have not been available for field measurements.

When deriving V_{cmax}, the choice of Rubisco kinetic parameters depends on how mesophyll conductance (g_m) is included (von Caemmerer *et al.*, 1994; Bernacchi *et al.*, 2002). If g_m is known, V_{cmax} can be derived from an $A \leftrightarrow C_c$ response curve. Kinetic parameters derived from tobacco are commonly used (K_c 272.4 µbar, K_o 165.8 mbar at 25°C) (Bernacchi *et al.*, 2002). If g_m is unknown, then V_{cmax} can be derived from an $A \leftrightarrow C_i$ response curve using 'apparent' Rubisco kinetic parameters (K_c 404.9 µbar, K_o 278.4 mbar at 25°C) (Bernacchi *et al.*, 2001). The C_c and C_i based approaches have been shown to closely describe CO_2 response curves in tobacco measured under a range of different oxygen partial pressures (von Caemmerer *et al.*, 1994) and temperatures (Bernacchi *et al.*, 2001, 2002). However, V_{cmax} estimates differed in some studies (Flexas *et al.*, 2007; Whitehead *et al.*, 2011). If the same set of constants are used to fit $A \leftrightarrow C_i$ and $A \leftrightarrow C_c$ curves, then one

obtains significantly lower V_{cmax} values on a C_i basis than on a C_c basis (Epron *et al.*, 1995; Manter & Kerrigan, 2004; Warren, 2008; Niinemets *et al.*, 2009a). The derived V_{cmax} values are highly sensitive to the values assumed for the kinetic constants (Medlyn *et al.*, 2002; Dietze, 2014). Unfortunately, these constants are not always explicitly stated. While the issue of selecting appropriate kinetic constants has been raised (Diaz-Espejo, 2013; Galmés *et al.*, 2016), few studies have compared V_{cmax} derived from both a C_i and C_c basis (Flexas *et al.*, 2007; Whitehead *et al.*, 2011; Nascimento & Marenco, 2013).

The draw-down in CO_2 partial pressure between intercellular airspaces and the sites of carboxylation in chloroplasts, C_i-C_c, reflects the balance between CO_2 assimilation rate and mesophyll conductance. An early survey of literature values found little difference in C_i-C_c between mesophytic and sclerophytic leaves (Evans, 1999; Evans & Loreto, 2000), but subsequent reviews that included leaves with very low photosynthetic capacity suggest that C_i-C_c increases when photosynthetic capacity is below 8 μmol m^{-2} s^{-1} and g_m is < 0.1 μmol m^{-2} s^{-1} bar^{-1}, indicating stronger mesophyll resistance (inverse of g_m) at low rates of photosynthesis (Ethier & Livingston, 2004; Warren & Adams, 2006; Niinemets *et al.*, 2009b; Tosens *et al.*, 2012). Given these observations, tropical trees exhibiting low photosynthetic rates might also exhibit stronger mesophyll resistance and larger C_i-C_c than temperate trees. Accounting for g_m might alter the estimate of V_{cmax} and reduce the difference in V_{cmax} per unit N between tropical and temperate trees. To our knowledge, the possibility of tropical leaves being more limited by mesophyll resistance than temperate leaves has not yet been investigated.

V_{cmax} is employed in at least eleven Earth system models to estimate global carbon fluxes and to simulate future global change (Rogers, 2014). In these models, empirical estimates of V_{cmax} are usually compiled from past studies; alternatively V_{cmax} could be inferred either from leaf N content/ fraction of N invested in Rubisco and leaf mass per area or from optimising photosynthesis and respiration (e.g. Cox, 2001; Krinner *et al.*, 2005; Kattge *et al.*, 2009; Friend, 2010; Bonan *et al.*, 2011). Almost all Earth system models assume infinite g_m and employ V_{cmax} on a C_i basis; however, Rogers *et al.* (2017) highlighted that failure to incorporate g_m when describing photosynthesis has the potential to create uncertainty in modelling terrestrial productivity. To address the increasing concern on the accuracy of FvCB model in estimating V_{cmax}, Sun *et al.* (2014b) proposed a hyperbolic function to convert V_{cmax} estimated on the basis of C_i to V_{cmax} estimated from C_c. The

smaller the value for g_m, the greater the divergence was between the two estimates of V_{cmax}. When this function was implemented into the Community Land Model CLM 4.5, there was a 16% increase in the estimate of global gross primary productivity from 1901 to 2010 (Sun *et al.*, 2014a). Given the critical role of V_{cmax} in modelling global carbon fluxes and the influence of g_m on the quantitative estimation of V_{cmax}, there is a need to expand datasets for V_{cmax} derived from A–C_c curves and to assess the accuracy of V_{cmax} estimation using a common approach (Rogers *et al.*, 2017).

Our objective was to compare photosynthetic properties of leaves from temperate and tropical forest trees including g_m, to determine if variation in g_m contributes to the difference in V_{cmax} per unit N that has been observed between these two groups. We calculated g_m directly from online isotope discrimination measurements made concurrently with gas exchange as described previously (Tazoe *et al.*, 2011; von Caemmerer & Evans, 2015). We used broadleaved evergreen species from thermally contrasting environments which are moist and non-freezing in order to minimise the potential impacts of co-variation in moisture stress and special adaptations needed to cope with freezing conditions (Xiang *et al.*, 2013).

Materials and Methods

Plant material and growth conditions

Seedlings of six evergreen tropical species originated from wet-forests of Queensland and five evergreen temperate species from cool-temperate wet-forests of Tasmania were sourced from commercial nurseries (see Table 1 for details on provenance and climate parameters at each provenance); these species were selected to represent thermally contrasting origins. Seedlings were 4–12 months old and 30–70 cm in height at the beginning of experiment. Seedlings were transplanted to 220-mm pots containing organic potting mixture and Osmocote® Exact standard controlled-release fertilizer (Scotts Australia, NSW, Australia) with an N : P : K ratio of 16 : 3.9 : 10 and grown in glasshouses in Canberra, Australia. The plants were grown under sufficient nutrient supply to minimise the impact of nutrient limitation (particularly phosphorus (P)) that usually occurs in warm environment, with none of the plants exhibiting visual symptoms of N and P deficiencies throughout the experiment. The glasshouse was controlled to achieve 25 : 20 °C, day : night to create favourable growth temperature for both tropical and temperate species alike and the plants were watered daily to

exceed pot capacity. Plants were arranged in four replicate blocks within the glasshouse, with each block containing randomly allocated individual of each species. The experiment took place in June–August 2015 (during which time the day length was 10 h) using natural light regime.

Leaf gas exchange and CO_2 response curve measurements

Leaf gas exchange measurements were made during June to August 2015, using two pairs of portable photosynthesis systems (Licor 6400XT infrared gas analyser, Li-Cor BioSciences, Lincoln, NE, USA). Measurements were made on the most recently fully expanded leaves developed in the glasshouse. Initial measurement was made at 400 µmol mol^{-1} of CO_2 concentrations inside the reference chamber, followed by a stepped sequence of 50, 100, 150, 250, 400, 600, 800, 1000, 1200 and finally 1500 µmol mol^{-1} to generate CO_2 response curves. The chamber block temperatures were set to 25 °C (leaf temperatures varied between 24.3 and 25.5 °C); photosynthetically active radiation (PAR) was 1500 µmol photons m^{-2} s^{-1} and O_2 was that of ambient air (i.e. fixed at 21%). $A \leftrightarrow C_i$ curves (examples shown in Fig. 1) were fitted following the model described by Farquhar *et al.* (1980) in order to calculate V_{cmax} and J_{1500} (rate of electron transport at 1500 µmol photons m^{-2} s^{-1}). V_{cmax} and J_{1500} values were determined via minimizing the sum of squares of modelled vs observed estimates of net CO_2 exchange at given CO_2 partial pressures at the site of the chloroplast (C_c). C_c was calculated from C_i (intercellular CO_2) assuming a constant value of mesophyll conductance, g_m, which was determined for each leaf (see the next section) in 2% O_2 to supress photorespiration. Rates of A at low CO_2 partial pressures were fitted to the Rubisco-limited equation of photosynthesis:

$$A = \left[\frac{V_{cmax}(C_c - \Gamma_*)}{\left(C_c + K_c\left(1 + {}^{O}/_{K_o}\right)\right)}\right] - R_{light} \qquad \text{Eqn 1}$$

where R_{light} is respiration in the light, Γ* is the CO_2 compensation point in the absence of photorespiration (36.9 µbar at 25°C; von Caemmerer *et al.* (1994)) and O is partial pressure of O_2. K_c and K_o are the effective Michaelis-Menten constants for CO_2 and O_2 at 25°C. If mesophyll conductance is known, C_c can be calculated and the values assumed for K_c and K_o were 260 µbar and 179 mbar, respectively, resulting in an effective K_m of 551 µbar at 25°C and O = 200mbar. When mesophyll conductance was ignored (i.e. g_m assumed to be infinite), Eqn 1 was fitted to C_i data assuming K_c and K_o to be 404 µbar and 248 mbar, respectively

(von Caemmerer *et al.*, 1994) resulting in an apparent K_m of 731 µbar at 25°C and O = 200mbar. R_{light} was estimated from the CO_2 response curve.

A cross validation between LI-6400XT instruments and 2 vs 21% O_2 measurements on the same leaf was made using Eqn 1. Having obtained V_{cmax} and R_{light} from the CO_2 response curve measured in 21% O_2, the Rubisco-limited CO_2 assimilation rate in 2% O_2 was calculated using the C_c value measured in 2% O_2.

Values for J_{1500} were calculated by fitting the electron-transport-limited equation of CO_2 assimilation to the CO_2 response curve at high CO_2 (generally when C_i > 500 µbar):

$$A = \left[\frac{J_{max}(C_c - \Gamma_*)}{(4C_c + 8\Gamma_*)}\right] - R_{light} \qquad \text{Eqn 2}$$

Concurrent gas exchange and carbon isotope discrimination measurements and calculation of mesophyll conductance

Gas exchange and carbon isotope discrimination measurements for the estimation of mesophyll conductance were made as described by Tazoe *et al.* (2011) and Evans & von Caemmerer (2013). A second pair of LI-6400XT gas exchange systems coupled to a tuneable diode laser (TDL; TGA100, Campbell Scientific, Inc., Logan, UT, USA) were used to make a second measurements on the same set of leaves, but in 2% O_2 and 380 µmol mol^{-1} of CO_2 (in leaf chamber). Reference and sample air were sampled via T junctions in the tubing for concurrent measurements of carbon isotope composition, with readings every 4 min. The flow rate was 200 µmol s^{-1}, irradiance 1500 µmol photons m^{-2} s^{-1} and leaf temperature controlled at 25°C. Air containing 2% O_2 was made by mixing N_2 and O_2 using mass flow controllers (Omega Engineering Inc., Stamford, CT, USA) and supplied to both the TDL system and the LI-6400 consoles and specified for the LI-6400 calculations. After *c*. 1 h of measurement in the light, respiration in the dark (R_{dark}) was measured for each leaf. Mesophyll conductance was calculated from carbon isotope discrimination with equations and fractionation factors described in Evans & von Caemmerer (2013). The ternary effects of transpiration rate on the rate of CO_2 assimilation through stomata were accounted for (Farquhar & Cernusak, 2012). The value of mesophyll conductance at 380 µmol mol^{-1} of CO_2 was used in the estimation on V_{cmax} from CO_2 response curve.

The limitations imposed by biochemistry, stomatal and mesophyll resistances to CO_2 diffusion on *A* were quantified based on the method published in Grassi & Magnani (2005), which were derived from *A*, stomatal conductance (g_s), g_m and V_{cmax}.

Leaf structural and nutrient measurements

Chlorophyll content was measured using a CCM-300 (Opti Science Inc., Hudson, NH, USA). Leaves were collected immediately after gas exchange and carbon isotope discrimination measurements were completed. Leaf areas were measured with a LI-3100C area meter (LiCor BioSciences, Lincoln, NE, USA) and leaf fresh masses were determined. Leaves were then placed in a drying oven at 60ºC for > 2 d and re-weighed to measure dry mass. Total leaf N and P concentrations were measured using Kjeldahl acid digest method, outlined in Ayub *et al.* (2011).

Statistical analysis

Statistical analyses were carried out using SPSS version 20 (IBM Corporation, NY, USA). Two-tailed, equal variance T-tests were used to compare overall means of tropical and temperate species. Comparisons were considered significant if $P<0.05$. Pearson correlations were used to measure bivariate relationships when tropical and temperate species analysed together. Standardized major axis (SMA) estimation was used to describe the best-fit relationship between pairs of variables and to assess whether relationships differed between tropical and temperate species, using SMATR Version 2.0 software (Falster *et al.*, 2006; Warton *et al.*, 2006).

Results

Cross-checking multiple gas exchange instruments

In our study, leaves were measured using two pairs of LI-6400 instruments. One pair was used to generate CO_2 response curves in 21% oxygen (O_2) while the other pair connected to a tuneable diode laser made measurements in 2% O_2 to suppress photorespiration. CO_2 response curves close to the mean response for tropical and temperate species are shown in Fig. 1. In general, photosynthetic rates of tropical and temperate species at ambient CO_2 were

Rubisco limited, as illustrated by the arrows. To cross-check the two instruments, a prediction of CO_2 assimilation rate in 2% O_2 with the internal CO_2 observed was made (see dotted lines in Fig. 1) from fitting the FvCB (1980) biochemical model to each CO_2 response curve measured in 21% O_2. Measured CO_2 assimilation rate in 2% O_2 (triangles in Fig. 1) aligned reasonably well with the predicted rates (dotted lines) in both cases, albeit with the 2% predicted values being slightly higher than that of the 2% measured values in this example. The comparison for all of the leaves is shown in Fig. 2. Predicted CO_2 assimilation rate in 2% O_2 correlated strongly with measured rate (P<0.01, r^2=0.95; Fig. 2) and – as was the case for the results in Fig. 1(b) – was generally slightly overestimated. The mean ratio of predicted to measured CO_2 assimilation rate in 2% O_2 was 1.11 ± 0.12 and 1.16 ± 0.19 for tropical and temperate trees, respectively, and the ranges of the two groups overlapped. This comparison suggested that there was no bias between the pairs of LI-6400s and that the FvCB (1980) model fitted both tropical and temperate trees**.**

Assimilation rate, mesophyll conductance and limitation to CO_2 assimilation rate

Strong positive correlations between photosynthetic rate at ambient CO_2 (A) and mesophyll conductance (g_m) were observed (P<0.05, r^2 = 0.74; Fig. 3a; Supporting Information Table S1). The tropical and temperate trees shared common A–g_m relationships as indicated by no significant difference in slope of the two groups (Table S2). The tropical trees occupied low ranges of A (4.5–14.3 µmol m^{-2} s^{-1}) and g_m (0.09–0.32 mol m^{-2} s^{-1} bar^{-1}) whereas the temperate trees were spread over larger ranges of A (5.4–27.3 µmol m^{-2} s^{-1}) and g_m (0.08–0.47 mol m^{-2} s^{-1} bar^{-1}).

The drawdown of CO_2 from the atmosphere to the sub-stomatal cavity (C_a–C_i) was independent of g_m (Fig. 3b, mean 103 µbar, P>0.05; Table S2). No distinct clustering of tropical and temperate trees was observed. At a given g_m, the drawdown of CO_2 in the gaseous phase imposed by stomatal resistance varied three-fold (49–173 µbar, Fig. 3b). The magnitude of the CO_2 drawdown from C_i to C_c was also independent of g_m (Fig. 3c, mean 55 µbar, P>0.05; Table S2), again with a three-fold range (30–95 µbar). The CO_2 drawdown from C_i to C_c was generally similar for tropical and temperate trees, overlapping for g_m ranging from 0.1 to 0.3 mol m^{-2} s^{-1} bar^{-1}. However, two temperate species, *A. moschatum* and *P. aspleniifolius*, exhibited larger drawdowns of CO_2 (71–95 µbar) at low g_m (0.08–0.13 mol m^{-2} s^{-1} bar^{-1}).

Comparison of V_{cmax} estimated with finite or infinite g_m

By calculating g_m from carbon isotope discrimination for each leaf, it was possible to estimate V_{cmax} on the basis of C_c assuming K_c and K_o values of 260 µbar and 179 mbar, respectively (von Caemmerer *et al.* (1994). Second, V_{cmax} was calculated on a C_i basis (assuming infinite g_m) using K_c and K_o of 404 µbar and 248 mbar, respectively (von Caemmerer *et al.*, 1994). V_{cmax} values calculated on a C_c basis were positively correlated with g_m (P<0.05, r^2 = 0.59; Fig. 4a). Tropical and temperate trees shared common slopes of A–g_m relationships (Table S2), although considerable scatter was observed. To investigate the consequences of the scatter, the lowest and highest deviation from the average V_{cmax} : g_m (indicated by squares) were analysed by assuming different values of g_m to estimate V_{cmax}. These simulations demonstrated that V_{cmax} decreased curvilinearly with increasing g_m (solid lines in Fig. 4b), declining steeply at the lower range of g_m (generally < 0.1 mol m^{-2} s^{-1} bar^{-1}, depending on species). The estimate of V_{cmax} for *L. leefeana*, a tropical species with the lowest V_{cmax} : g_m (133), was less sensitive to decreasing g_m than *P. aspleniifolius* which had the greatest V_{cmax} : g_m (551). The value of V_{cmax} estimated on the basis of C_i is represented by dashed lines in Fig. 4(b). The greater V_{cmax} : g_m for *P. aspleniifolius* resulted in a steeper increase in V_{cmax} as g_m was reduced below 0.2 mol m^{-2} s^{-1} bar^{-1} compared to *L. leefeana* and meant that V_{cmax} estimated on the basis of C_i would have underestimated the true value of *P. aspleniifolius* by 30% (Fig. 4b). A pattern to describe the consequence of variations in V_{cmax} : g_m to estimation of V_{cmax} on C_c and C_i basis was found. For the species reported here, a V_{cmax} : g_m ratio of 218 yielded similar estimates of V_{cmax} on C_c and C_i basis (see dashed line in Fig. 4a). For data points distributed close to the dotted line (extrapolated from the lowest point *L. leefeana* illustrated in Fig. 4b), V_{cmax}–C_i values exceeded V_{cmax}–C_c values by *c*. 3–5%. For data points in proximity to the solid line (extrapolated from the highest point *P. aspleniifolius* illustrated in Fig. 4b), V_{cmax}–C_i values were *c*. 20% less than V_{cmax}–C_c depicted in Fig. 5.

V_{cmax} estimated on a C_i basis was generally similar to the actual V_{cmax}–C_c (Table 2; Fig. 5), despite the variations in V_{cmax} : g_m ratio. Although the tropical and temperate trees shared a common slope between V_{cmax}–C_c and V_{cmax}–C_i (Table S2), the deviation between V_{cmax}–C_i and V_{cmax}–C_c was slightly greater for temperate trees (12% vs 5% for temperate and tropical means, respectively (Table 2)). Temperate tree means for V_{cmax}–C_c and V_{cmax}–C_i were 80 ± 32 and 72 ± 29 µmol m^{-2} s^{-1}, respectively; tropical tree means were 48 ± 15 and 45 ± 13 µmol m^{-2} s^{-1}, respectively. The overall ratio of J_{1500} estimated on C_c over C_i basis was 1.05 ± 0.01 for tropical and temperate groups (data not shown).

Comparison of tropical and tropical leaf traits

The overall mean value of A in tropical trees (8.6 ± 2.7 µmol m^{-2} s^{-1}) was almost half that of temperate trees (14.3 ± 6.9 µmol m^{-2} s^{-1}; Table 2). While leaf mass per area (LMA) was also lower in tropical trees, the difference in A was maintained when expressing rates on a dry mass basis (data not shown). Lower overall rate of ambient photosynthesis in tropical trees was accompanied by significantly lower stomatal conductance (g_s), as well as lower underpinning biochemical capacities, shown here as V_{cmax} and J_{1500} (electron transport rate at 1500 µmol photons m^{-2} s^{-1}) in comparison to temperate trees (P<0.05; Table 2).

Estimation of the relative limitations imposed by biochemistry, stomatal and mesophyll resistances on A for each species are presented in Fig. 6. In general, limitations by mesophyll (L_m) contributed to the smallest fraction (approximately a quarter) of total limitations to A. In tropical species, L_m values were relatively constant whilst stomatal limitations (L_s) and biochemical limitations (L_b) varied. In temperate species, L_s and L_m increased with decreasing A, with *E. lucida* showing the highest L_s. L_m and L_s imposed similar limitations to A in *E. obliqua, P. apetala and A. moschatum*. No relationship between L_b and any photosynthetic parameter was observed between species.

Comparison of tropical and temperate species at low range of A (i.e. excluding *E. obliqua* and *P. apetala*) showed that mean L_s were similar between the two groups. At low A (8.6 ± 2.7 and 9.1 ± 2.1 µmol m^{-2} s^{-1} for tropical and temperate, respectively; P>0.05), mean L_s were *c.* 0.44 ± 0.14 for both groups. Mean L_m were significantly higher in temperate species than in tropical species (0.29 ± 0.06 and 0.19 ± 0.05 for temperate and tropical, respectively; P<0.05). By contrast, tropical species exhibited higher L_b than those of temperate species (0.37 ± 0.16 and 0.27 ± 0.09 for temperate and tropical, respectively; P<0.05).

As expected, V_{cmax} and J_{1500} co-varied on both area and mass bases (Fig. 7; Table S2). There was a significant difference in the slope of $V_{cmax} \leftrightarrow J_{1500}$ relationships between topical and temperate trees on area and mass bases (Table S2). However, the overall mean ratio of J_{1500} to V_{cmax} was not significantly different between tropical and temperate trees (P>0.05, 1.71 ± 0.24 and 1.74 ± 0.27, respectively).

In our study, the range of leaf mass per area (LMA) was slightly constrained (32–118 g m^{-2}). A weak negative correlation between photosynthetic N-use efficiency (V_{cmax} per unit leaf N) and LMA was found only for temperate trees (Fig. 8; Table S2). Tropical trees had lower V_{cmax} per unit leaf N for a given LMA than the temperate trees (Fig. 8, 30.4 ± 7.6 and

42.2 ± 15.8 µmol CO_2 gN^{-1} s^{-1} for tropical and temperate trees, respectively). Values for V_{cmax} per unit leaf N for tropical and temperate species generally fell below and above the mean function fitted to the GLOPNET data (Hikosaka, 2004; Wright *et al.*, 2004). The N and P contents were both less for tropical compared to temperate leaves ($P<0.05$; Table 1).

Discussion

The diversity of plant species, particularly in tropical biomes, precludes having detailed information about each and thus Earth system models make simplifying assumptions. The parameterisation of maximum Rubisco activity, $V_{cmax,}$ as a function of leaf N and leaf mass per area with respect to plant functional type and biome (e.g. tropical evergreen/ deciduous trees, temperate evergreen/ needle trees) has been shown to reduce uncertainties in model outputs (Kattge *et al.*, 2009; Alton, 2011), but require several assumptions about the underlying biochemistry (Rogers, 2014; Rogers *et al.*, 2017). Here, we addressed one of these key assumptions: can V_{cmax} be estimated while ignoring mesophyll conductance (g_m)? Two issues arise. First, does the rate of CO_2 assimilation predicted from leaf N concentration and leaf mass per area reflect rates observed in the field? Second, how robust are the predictions as one moves away from current conditions? The experimental data presented here were designed to investigate the impact of g_m on modelling the rate of CO_2 assimilation.

The original formulation of the FvCB model requires the CO_2 partial pressure in the chloroplast stroma. Conventional gas exchange measurements allow the calculation of the intercellular CO_2 partial pressure (C_i) and it was argued that the drawdown between C_i and C_c (chloroplastic CO_2 partial pressure) was sufficiently small that it could be ignored (i.e. $C_c = C_i$). CO_2 response curves of photosynthesis have been measured on a wide range of species in the field (Kattge *et al.*, 2011) as portable gas exchange instruments became readily available. With progress in methods to estimate g_m, it is now clear that there is a significant drawdown in the partial pressure of CO_2 within the mesophyll (Evans *et al.*, 1986; von Caemmerer & Evans, 1991; Harley *et al.*, 1992; Loreto *et al.*, 1992; Pons *et al.*, 2009) and Fig. 3(c). However, mesophyll conductance has generally not been measured during field observations. Although it is now possible to measure chlorophyll fluorescence in conjunction with conventional gas exchange with commercially available instruments, there is a trade-off associated with the smaller leaf chamber used when measuring fluorescence, which compromises the accuracy of the gas exchange measurements.

The derivation of V_{cmax}–C_c and V_{cmax}–C_i requires the use of different values for Michaelis Menten constants for CO_2 and O_2 (K_c and K_o, respectively) in each case ('true' values for the former and 'apparent' values for the latter). In the absence of g_m, V_{cmax} can be estimated from the response of A to C_i by assuming an apparent K_m for Rubisco to represent K_c (1+O/K_o). Using an apparent K_m to estimate V_{cmax} is a useful approach if the drawdown C_i-C_c is similar between species (Warren, 2008). Moreover, in order for the estimate of V_{cmax}–C_i to match V_{cmax}–C_c, the ratio of V_{cmax}–C_c to g_m needs to be similar to that of tobacco as the relationship between apparent $K_{c(\infty)}$ and the true K_c is $K_{c\ (\infty)} = K_c + V_{cmax}/g_m$ (Eqn 14 in von Caemmerer *et al.* (1994)). Upon reanalysis of published A↔C_i curves for many species, Ethier & Livingston (2004) suggest that V_{cmax} and g_m are not closely related to each other and therefore it is inappropriate to apply a single value for the apparent K_m. Sun *et al.* (2014b) took a similar approach of deriving V_{cmax} from A↔C_i curves while allowing the apparent K_m to vary and compared this to V_{cmax}–C_c which was obtained by deriving a value for g_m from the curvature of A↔C_i response. They found that on average, V_{cmax}–C_i was only 68% of V_{cmax}–C_c. However, in both of these cases, there were no direct measurements of g_m. So, the question is, does one reach the same conclusion when g_m and CO_2 response curves are directly measured?

Although we only measured 11 evergreen tree species here, the derived estimates of V_{cmax} ranged from 25 to 150 µmol m^{-2} s^{-1} which encompasses the majority of the range reported by Ali *et al.* (2015). Our key result is that by calculating g_m from concurrent measurements of carbon isotope discrimination, we could directly compare V_{cmax}–C_c against V_{cmax}–C_i. We observed much closer agreement (Fig. 5) than previous comparisons which derive g_m from analysis of CO_2 response curves (Ethier & Livingston, 2004; Warren, 2008; Sun *et al.*, 2014b). We confirmed the finding that V_{cmax} and V_{cmax} per unit N are greater for temperate than tropical evergreen trees (Figs 7,8; Kattge *et al.*, 2009; Xiang *et al.*, 2013; Ali *et al.*, 2015) and demonstrate that this is not confounded by deriving V_{cmax} on the basis of intercellular CO_2 partial pressure using a fixed apparent K_m. Our use of isotope discrimination to measure g_m necessitated the use of young plants grown in pots in glasshouses. Although the properties of such leaves may differ from adult trees growing in their natural forest environment, we observed differences between temperate and tropical evergreen tree species consistent with measurements made on leaves in the field (Kattge *et al.*, 2009; Ali *et al.*, 2015) although V_{cmax} values as low as 15–20 µmol m^{-2} s^{-1} have been reported for two central Amazonian species (Nascimento & Marenco, 2013).

Extending predictions away from current conditions

The power of basing models of ecosystem productivity on the FvCB model is that it captures the underlying biochemistry centred around the kinetic properties of Rubisco. This allows succinct description of the responses to CO_2 and temperature. The FvCB model has been extensively verified against leaf gas exchange measurements for many species. However, a key assumption is the use of Rubisco kinetic parameters determined for tobacco to represent all C_3 species. The lack of complete suites of Rubisco parameters including temperature responses currently precludes models being able to capture or represent this complexity.

Recently attention has been focussed on whether mesophyll conductance needs to be included (Rogers *et al.*, 2017). Sun *et al.* (2014b) reanalysed 1000 $A{\leftrightarrow}C_i$ curves from 130 species, using the same K_m (CO_2) to derive estimates of V_{cmax}–C_i, V_{cmax}–C_c and g_m from which they proposed a function relating V_{cmax}–C_i to V_{cmax}–C_c and g_m. Subsequently this function was implemented into a community land model to assess the impact on gross primary productivity (GPP) from 1901 to 2010 (Sun *et al.*, 2014a). They suggest that including g_m would increase the CO_2 fertilization effect by 16% over that period. By contrast, we derived V_{cmax}–C_c and V_{cmax}–C_i values assuming a 'true' K_m (CO_2) or a constant 'apparent' K_m (CO_2), respectively. Our two estimates of V_{cmax} were nearly the same (Table 2; Fig. 5). As our approach differs from that of Sun *et al.* (2014b), we re-examined the implication for modelling CO_2 assimilation rate as atmospheric partial pressure of CO_2 changes. We illustrate the difference between parameters derived using intercellular or chloroplastic partial pressure of CO_2 when g_m is known. The mean values for temperate tree species were used (Table 2) as this group had the largest difference between V_{cmax}–C_c and V_{cmax}–C_i and therefore represents the worst case scenario. The CO_2 response curves generated using both sets of values are shown against C_i (Fig. 9). While both curves overlay closely for C_i between 100–200 µbar, the curve including g_m has a greater rate of CO_2 assimilation at a C_i of 300 µbar, reflecting the lower K_m value (551 vs 731, for C_c and C_i scenarios, respectively). There is a complicated response to C_i for the difference between the two scenarios (Fig. 9). CO_2 assimilation rate predicted on the basis of C_c exceeds that based on C_i, reaching a maximum of 4% at the transition (332 µbar), then declined to a minimum of -5% at the transition point for the C_i based scenario (428 µbar) before finally returning to similarity at 650 µbar. If one assumes a C_i : C_a ratio of 0.7, then simulating GPP as C_a increased from 300 to 390 µbar represents C_i increasing from 210 to 273 µbar and CO_2

assimilation would have been underestimated by between 1–3% using C_i based rather than C_c based parameters. For C_a = 390 ppm, Sun *et al.* (2014a) estimated the CO_2 fertilization effect was underestimated by 4.5 Pg C p.a. over a baseline GPP of 127 Pg C p.a., i.e. *c*. 3.5%. Thus our estimate of the impact of including g_m when forecasting the change in CO_2 assimilation as atmospheric CO_2 concentration rises is similar but slightly less than that of Sun *et al.* (2014a).

Admittedly the analysis here is very simplistic and ignores the influence of temperature. It is known that the temperature response of g_m varies considerably between species (von Caemmerer & Evans, 2015) and it has been recognised that different temperature responses for g_m would significantly impact on model predictions of CO_2 assimilation rate (Warren, 2008; Rogers *et al.*, 2017). While incorporating g_m into models to estimate GPP is theoretically appealing, in practice it is not yet possible as it requires knowledge of Rubisco kinetic parameters for a range of evergreen tree species, an estimate of g_m and its temperature response for representative species, as well as functions relating V_{cmax} to leaf N content per unit leaf area.

Photosynthetic capacity scaled with g_m in tropical and temperate evergreen trees

The strong correlations between photosynthetic rate and g_m for both tropical and temperate trees (Fig. 3a; Table S1) are consistent with previous studies on a range of species (Epron *et al.*, 1995; Evans & Loreto, 2000; Flexas *et al.*, 2008; Whitehead *et al.*, 2011; Tosens *et al.*, 2012). Tropical and temperate species shared a common relationship between photosynthetic capacity and g_m (Figs 3a, 4a) which meant that there was little variation in the drawdown from C_i to C_c (Fig. 3c; Table S1). This contrasts with past observations of a greater mesophyll drawdown (C_i-C_c) for leaves with low photosynthetic capacity (Ethier & Livingston, 2004; Warren & Adams, 2006; Niinemets *et al.*, 2009b; Tosens *et al.*, 2012). The low photosynthetic rates of tropical trees we observed are not due to low C_c values relative to temperate species.

Our average of C_i–C_c, 55 µbar, is consistent with values for tree species measured recently using the same instrument (von Caemmerer & Evans, 2015) but lower than those compiled earlier: 83–91 µbar (Evans & Loreto, 2000; Warren, 2008; Buckley & Warren, 2014). The range of g_m values, 0.08–0.47 mol m^{-2} s^{-1} bar^{-1}, is comparable to past studies (Pons & Welschen, 2003; Flexas *et al.*, 2008; Whitehead *et al.*, 2011; von Caemmerer &

Evans, 2015). The greater drawdown imposed by stomata, C_a–C_i (average of 103 µbar) matches the average for woody evergreen (Warren, 2008) and tree species (von Caemmerer & Evans, 2015), 109 µbar.

The average values of g_m across woody evergreen, woody deciduous and conifers reported in the literature are close to 0.1 mol m^{-2} s^{-1} bar^{-1} (Flexas *et al.*, 2008; Buckley & Warren, 2014). This might indicate that in these plant groups, it is more likely that estimates of V_{cmax}–C_c differ from V_{cmax}–C_i. In addition, water-stressed plants exhibit greater mesophyll drawdowns from C_i to C_c (Flexas *et al.*, 2006; Warren, 2008; Niinemets *et al.*, 2009b). However, it becomes more difficult to measure g_m on leaves with low photosynthetic rates. As the values of g_m in our study were larger than 0.1 mol m^{-2} s^{-1} bar^{-1}, our conclusions may not extend into this lower bound region where much larger mesophyll drawdowns have been reported (Warren, 2008; Niinemets *et al.*, 2009b). A definitive assessment of this issue will require further work focusing on very low range of g_m and validation on the interactive effects of internal and stomatal conductances in influencing water stress responses.

Photosynthetic performance with respect to nitrogen and phosphorus

Meta-analyses of field surveys have reported smaller values of V_{cmax}–C_i for tropical than temperate trees (41 vs 61 µmol CO_2 m^{-2} s^{-1}, respectively (Kattge *et al.*, 2009) and 30 vs 80 µmol CO_2 m^{-2} s^{-1}, respectively (Ali *et al.*, 2015)), similar to what we observed (48 and 80 µmol CO_2 m^{-2} s^{-1} for tropical and temperate species, respectively, Table 2). In addition, tropical trees have smaller values of V_{cmax} per unit N (tropical vs temperate: 22 vs 34 µmol CO_2 gN^{-1} s^{-1} (Kattge *et al.*, 2009), 20 vs 40 µmol CO_2 gN^{-1} s^{-1} (Ali *et al.*, 2015), 31 vs 42; Tables 1, 2).

Tropical and temperate species shared a similar range in leaf mass per area. Consequently, the low V_{cmax} per unit N of tropical species (Fig. 8) does not reflect a trade-off against structural N (Onoda *et al.*, 2017). The lower V_{cmax} per unit N of tropical species could reflect less leaf N allocated to photosynthetic proteins. This was suggested in comparisons between plants adapted to warm and cool environments, in both field and glasshouse settings (Xiang *et al.*, 2013; Ali *et al.*, 2015; Dusenge *et al.*, 2015; Bahar *et al.*, 2017; Scafaro *et al.*, 2017). In turn, this implies that a greater fraction of leaf N could be allocated to non-photosynthetic components (e.g. cell wall N and/or defence compounds) in warm-adapted species, reflecting trade-offs associated with leaf longevity and herbivory resistance in warm

environment (Kikuzawa *et al.*, 2013; Metcalfe *et al.*, 2014). Alternatively, the kinetic properties of Rubisco, or its activation state could differ between tropical and temperate species. Our plants were supplied with fertilizer which resulted in leaf P concentrations almost double that observed for leaves of these Australian species sampled in the field (K. J. Bloomfield & O. K. Atkin, unpublished) or for several Amazonian tree species (Mendes & Marenco, 2015). We tried to avoid nutrient deficiency complicating our results, but if P deficiency affected g_m, then potentially this could alter the estimation of V_{cmax}. Due to the smaller LMA of our glasshouse grown plants compared to leaves sampled in the field in South America (Bahar *et al.*, 2017; Norby *et al.*, 2017), the P contents per unit leaf area overlapped. Having largely ruled out g_m as a possible contributor, attention should be focussed on obtaining more detailed information about Rubisco in these species.

Conclusion

Leaves from evergreen tropical tree seedlings have lower rates of photosynthesis and underpinning biochemistry than their temperate counterparts. For both tropical and temperate species, estimates of V_{cmax}–C_i closely matched those of V_{cmax}–C_c which were based on g_m derived from ^{13}C discrimination measurements. A single value for the apparent K_m could be assumed because the ratio of V_{cmax} : g_m was relatively constant. The lower photosynthetic capacity of tropical leaves was associated with a smaller V_{cmax} per unit leaf N and less N per unit leaf area.

ACKNOWLEDGMENTS

This work was funded by grants from the Australian Research Council (DP130101252) to O.K.A. and supported by the ARC Centre of Excellence in Plant Energy Biology (CE140100008), and ARC Centre of Excellence for Translational Photosynthesis. N.H.A.B. was funded by a Malaysian Government Postgraduate Scholarship. We thank Lingling Zhu for sharing plant materials.

AUTHOR CONTRIBUTIONS

N.H.A.B., O.K.A. and J.R.E. planned and designed the research. N.H.A.B., J.R.E., L.H. collected and analysed data. N.H.A.B., J.R.E., A.P.S. and O.K.A. interpreted data and wrote the manuscript.

References

Ali AA, Xu C, Rogers A, McDowell NG, Medlyn BE, Fisher RA, Wullschleger SD, Reich PB, Vrugt JA, Bauerle WL*, et al.* 2015. Global-scale environmental control of plant photosynthetic capacity. *Ecological Applications* **25**: 2349-2365.

Alton PB. 2011. How useful are plant functional types in global simulations of the carbon, water, and energy cycles? *Journal of Geophysical Research: Biogeosciences* **116:** G01030.

Atkin OK, Bloomfield KJ, Reich PB, Tjoelker MG, Asner GP, Bonal D, Bönisch G, Bradford MG, Cernusak LA, Cosio EG *et al.* 2015. Global variability in leaf respiration in relation to climate, plant functional types and leaf traits. *New Phytologist* **206**: 614–636.

Ayub G, Smith RA, Tissue DT, Atkin OK. 2011. Impacts of drought on leaf respiration in darkness and light in *Eucalyptus saligna* exposed to industrial-age atmospheric CO_2 and growth temperature. *New Phytologist* **190**: 1003-1018.

Bahar NHA, Ishida FY, Weerasinghe LK, Guerrieri R, O'Sullivan OS, Bloomfield KJ, Asner GP, Martin RE, Lloyd J, Malhi Y *et al.* 2017. Leaf-level photosynthetic capacity in lowland Amazonian and high-elevation Andean tropical moist forests of Peru. *New Phytologist* **214**: 1002–1018.

Bernacchi CJ, Portis AR, Nakano H, von Caemmerer S, Long SP. 2002. Temperature response of mesophyll conductance. Implications for the determination of Rubisco enzyme kinetics and for limitations to photosynthesis *in vivo*. *Plant Physiology* **130**: 1992-1998.

Bernacchi CJ, Singsaas EL, Pimentel C, Portis Jr AR, Long SP. 2001. Improved temperature response functions for models of Rubisco-limited photosynthesis. *Plant, Cell & Environment* **24**: 253-259.

Bonan GB. 2008. Forests and climate change: forcings, feedbacks, and the climate benefits of forests. *Science* **320**: 1444.

Bonan GB, Lawrence PJ, Oleson KW, Levis S, Jung M, Reichstein M, Lawrence DM, Swenson SC. 2011. Improving canopy processes in the Community Land Model version 4 (CLM4) using global flux fields empirically inferred from FLUXNET data. *Journal of Geophysical Research: Biogeosciences* **116**: G02014.

Buckley TN, Warren CR. 2014. The role of mesophyll conductance in the economics of nitrogen and water use in photosynthesis. *Photosynthesis Research* **119**: 77-88.

Cox PM. 2001. *Description of the TRIFFID dynamic global vegetation model: Technical Note 24.* Bracknell, UK: Hadley Centre, United Kingdom Meteorological Office.

Diaz-Espejo A. 2013. New challenges in modelling photosynthesis: temperature dependencies of Rubisco kinetics. *Plant, Cell & Environment* **36**: 2104-2107.

Dietze MC. 2014. Gaps in knowledge and data driving uncertainty in models of photosynthesis. *Photosynthesis Research* **119**: 3-14.

Dusenge M, Wallin G, Gårdesten J, Niyonzima F, Adolfsson L, Nsabimana D, Uddling J. 2015. Photosynthetic capacity of tropical montane tree species in relation to leaf nutrients, successional strategy and growth temperature. *Oecologia* **177**: 1183-1194.

Epron D, Godard D, Cornic G, Genty B. 1995. Limitation of net CO_2 assimilation rate by internal resistances to CO_2 transfer in the leaves of two tree species (*Fagus sylvatica* L. and *Castanea sativa* Mill.). *Plant, Cell & Environment* **18**: 43-51.

Ethier GJ, Livingston NJ. 2004. On the need to incorporate sensitivity to CO_2 transfer conductance into the Farquhar–von Caemmerer–Berry leaf photosynthesis model. *Plant, Cell & Environment* **27**: 137-153.

Evans J, Sharkey T, Berry J, Farquhar G. 1986. Carbon isotope discrimination measured concurrently with gas exchange to investigate CO_2 diffusion in leaves of higher plants. *Functional Plant Biology* **13**: 281-292.

Evans JR. 1989. Photosynthesis and nitrogen relationships in leaves of C_3 plants. *Oecologia* **78**: 9-19.

Evans JR. 1999. Leaf anatomy enables more equal access to light and CO_2 between chloroplasts. *New Phytologist* **143**: 93-104.

Evans JR, Loreto F. 2000. Acquisition and diffusion of CO_2 in higher plant leaves. In: Leegood RC, Sharkey TD, von Caemmerer S, eds. *Photosynthesis: physiology and metabolism*. Dordrecht, the Netherlands: Springer Netherlands, 321-351.

Evans JR, Von Caemmerer S. 2013. Temperature response of carbon isotope discrimination and mesophyll conductance in tobacco. *Plant, Cell & Environment* **36**: 745-756.

Falster DS, Warton DI, Wright IJ. 2006. SMATR: Standardised major axis tests and routines, version 2.0. [WWW document] URL https://github.com/dfalster/smatr/.

Farquhar GD, Caemmerer S, Berry JA. 1980. A biochemical model of photosynthetic CO_2 assimilation in leaves of C_3 species. *Planta* **149**: 78-90.

Farquhar GD, Cernusak LA. 2012. Ternary effects on the gas exchange of isotopologues of carbon dioxide. *Plant, Cell & Environment* **35**: 1221-1231.

Flexas J, Bota J, Galmés J, Medrano H, Ribas-Carbó M. 2006. Keeping a positive carbon balance under adverse conditions: responses of photosynthesis and respiration to water stress. *Physiologia Plantarum* **127**: 343-352.

Flexas J, Díaz-Espejo A, Berry J, Cifre J, Galmés J, Kaldenhoff R, Medrano H, Ribas-Carbó M. 2007. Analysis of leakage in IRGA's leaf chambers of open gas exchange systems: quantification

and its effects in photosynthesis parameterization. *Journal of Experimental Botany* **58**: 1533-1543.

Flexas J, Ribas-Carbó M, Diaz-Espejo A, Galmés J, Medrano H. 2008. Mesophyll conductance to CO_2: current knowledge and future prospects. *Plant, Cell & Environment* **31**: 602-621.

Friend AD. 2010. Terrestrial plant production and climate change. *Journal of Experimental Botany* **61**: 1293–1309.

Galmés J, Hermida-Carrera C, Laanisto L, Niinemets Ü. 2016. A compendium of temperature responses of Rubisco kinetic traits: variability among and within photosynthetic groups and impacts on photosynthesis modeling. *Journal of Experimental Botany* **67**: 5067-5091.

Grassi G, Magnani F. 2005. Stomatal, mesophyll conductance and biochemical limitations to photosynthesis as affected by drought and leaf ontogeny in ash and oak trees. *Plant, Cell & Environment* **28**: 834-849.

Harley PC, Thomas RB, Reynolds JF, Strain BR. 1992. Modelling photosynthesis of cotton grown in elevated CO_2. *Plant, Cell & Environment* **15**: 271-282.

Hijmans RJ, Cameron SE, Parra JL, Jones PG, Jarvis A. 2005. Very high resolution interpolated climate surfaces for global land areas. *International Journal of Climatology* **25**: 1965-1978.

Hikosaka K. 2004. Interspecific difference in the photosynthesis–nitrogen relationship: patterns, physiological causes, and ecological importance. *Journal of Plant Research* **117**: 481-494.

Hikosaka K, Hanba YT, Hirose T, Terashima I. 1998. Photosynthetic nitrogen-use efficiency in leaves of woody and herbaceous species. *Functional Ecology* **12**: 896-905.

Kattge J, Díaz S, Lavorel S, Prentice IC, Leadley P, Bönisch G, Garnier E, Westoby M, Reich PB, Wright IJ *et al.* 2011. TRY – a global database of plant traits. *Global Change Biology* **17**: 2905-2935.

Kattge J, Knorr W, Raddatz T, Wirth C. 2009. Quantifying photosynthetic capacity and its relationship to leaf nitrogen content for global-scale terrestrial biosphere models. *Global Change Biology* **15**: 976-991.

Kikuzawa K, Onoda Y, Wright IJ, Reich PB. 2013. Mechanisms underlying global temperature-related patterns in leaf longevity. *Global Ecology and Biogeography* **22**: 982-993.

Krinner G, Viovy N, de Noblet-Ducoudré N, Ogée J, Polcher J, Friedlingstein P, Ciais P, Sitch S, Prentice IC. 2005. A dynamic global vegetation model for studies of the coupled atmosphere-biosphere system. *Global Biogeochemical Cycles* **19:** GB1015.

Loreto F, Harley PC, Di Marco G, Sharkey TD. 1992. Estimation of mesophyll conductance to CO_2 flux by three different methods. *Plant Physiology* **98**: 1437-1443.

Manter DK, Kerrigan J. 2004. A/C_i curve analysis across a range of woody plant species: influence of regression analysis parameters and mesophyll conductance. *Journal of Experimental Botany* **55**: 2581-2588.

Medlyn BE, Dreyer E, Ellsworth D, Forstreuter M, Harley PC, Kirschbaum MUF, Le Roux X, Montpied P, Strassemeyer J, Walcroft A *et al.* 2002. Temperature response of parameters of a biochemically based model of photosynthesis. II. A review of experimental data. *Plant, Cell & Environment* **25**: 1167-1179.

Mendes KR, Marenco RA. 2015. Photosynthetic traits of tree species in response to leaf nutrient content in the central Amazon. *Theoretical and Experimental Plant Physiology* **27**: 51-59.

Metcalfe DB, Asner GP, Martin RE, Silva Espejo JE, Huasco WH, Farfán Amézquita FF, Carranza-Jimenez L, Galiano Cabrera DF, Baca LD, Sinca F *et al.* 2014. Herbivory makes major contributions to ecosystem carbon and nutrient cycling in tropical forests. *Ecology Letters* **17**: 324-332.

Nascimento HCS, Marenco RA. 2013. Mesophyll conductance variations in response to diurnal environmental factors in *Myrcia paivae* and *Minquartia guianensis* in Central Amazonia. *Photosynthetica* **51**: 457-464.

Niinemets Ü, Díaz-Espejo A, Flexas J, Galmés J, Warren CR. 2009a. Importance of mesophyll diffusion conductance in estimation of plant photosynthesis in the field. *Journal of Experimental Botany* **60**: 2271-2282.

Niinemets Ü, Díaz-Espejo A, Flexas J, Galmés J, Warren CR. 2009b. Role of mesophyll diffusion conductance in constraining potential photosynthetic productivity in the field. *Journal of Experimental Botany* **60**: 2249–2270.

Norby RJ, Gu L, Haworth IC, Jensen AM, Turner BL, Walker AP, Warren JM, Weston DJ, Xu C, Winter K. 2017. Informing models through empirical relationships between foliar phosphorus, nitrogen and photosynthesis across diverse woody species in tropical forests of Panama. *New Phytologist* **215**: 1425-1437.

Onoda Y, Wright IJ, Evans JR, Hikosaka K, Kitajima K, Niinemets Ü, Poorter H, Tosens T, Westoby M. 2017. Physiological and structural tradeoffs underlying the leaf economics spectrum. *New Phytologist* **214**: 1447–1463.

Pan Y, Birdsey RA, Fang J, Houghton R, Kauppi PE, Kurz WA, Phillips OL, Shvidenko A, Lewis SL, Canadell JG *et al.* 2011. A large and persistent carbon sink in the world's forests. *Science* **333**: 988-993.

Pons TL, Flexas J, von Caemmerer S, Evans JR, Genty B, Ribas-Carbo M, Brugnoli E. 2009. Estimating mesophyll conductance to CO_2: methodology, potential errors, and recommendations. *Journal of Experimental Botany* **60**: 2217–2234.

Pons TL, Welschen RAM. 2003. Midday depression of net photosynthesis in the tropical rainforest tree *Eperua grandiflora*: contributions of stomatal and internal conductances, respiration and Rubisco functioning. *Tree Physiology* **23**: 937-947.

Prentice IC, Harrison SP, Bartlein PJ. 2011. Global vegetation and terrestrial carbon cycle changes after the last ice age. *New Phytologist* **189**: 988-998.

Rogers A. 2014. The use and misuse of *Vc,max* in Earth System Models. *Photosynthesis Research* **119**: 15-29.

Rogers A, Medlyn BE, Dukes JS, Bonan G, von Caemmerer S, Dietze MC, Kattge J, Leakey ADB, Mercado LM, Niinemets Ü *et al.* 2017. A roadmap for improving the representation of photosynthesis in Earth system models. *New Phytologist* **213**: 22-42.

Scafaro AP, Xiang S, Long BM, Bahar NHA, Weerasinghe KWLK, Creek D, Evans JR, Reich PB, Atkin OK. 2017. Strong thermal acclimation of photosynthesis in tropical and temperate wet-forest tree species: the importance of altered Rubisco content. *Global Change Biology* **23**: 2783–2800.

Sun Y, Gu L, Dickinson RE, Norby RJ, Pallardy SG, Hoffman FM. 2014a. Impact of mesophyll diffusion on estimated global land CO_2 fertilization. *Proceedings of the National Academy of Sciences, USA* **111**: 15774-15779.

Sun Y, Gu L, Dickinson RE, Pallardy SG, Baker J, Cao Y, Damatta FM, Dong X, Ellsworth D, Van Goethem D*, et al.* 2014b. Asymmetrical effects of mesophyll conductance on fundamental photosynthetic parameters and their relationships estimated from leaf gas exchange measurements. *Plant, Cell & Environment* **37**: 978-994.

Tazoe Y, Von Caemmerer S, Estavillo GM, Evans JR. 2011. Using tunable diode laser spectroscopy to measure carbon isotope discrimination and mesophyll conductance to CO_2 diffusion dynamically at different CO_2 concentrations. *Plant, Cell & Environment* **34**: 580-591.

Tosens T, Niinemets Ü, Vislap V, Eichelmann H, Castro DÍez P. 2012. Developmental changes in mesophyll diffusion conductance and photosynthetic capacity under different light and water availabilities in *Populus tremula*: how structure constrains function. *Plant, Cell & Environment* **35**: 839-856.

Verheijen L, Brovkin V, Aerts R, Bönish G, Cornelissen J, Kattge J, Reich P, Wright I, Van Bodegom P. 2013. Impacts of trait variation through observed trait-climate relationships on

performance of a representative Earth System model: a conceptual analysis. *Biogeosciences* **10**: 5497-5515.

von Caemmerer S, Evans J. 1991. Determination of the average partial pressure of CO_2 in chloroplasts fom leaves of several C_3 plants. *Functional Plant Biology* **18**: 287-305.

von Caemmerer S, Evans JR. 2015. Temperature responses of mesophyll conductance differ greatly between species. *Plant, Cell & Environment* **38**: 629-637.

von Caemmerer S, Evans JR, Hudson GS, Andrews TJ. 1994. The kinetics of ribulose-1, 5-bisphosphate carboxylase/oxygenase *in vivo* inferred from measurements of photosynthesis in leaves of transgenic tobacco. *Planta* **195**: 88-97.

Warren CR. 2008. Stand aside stomata, another actor deserves centre stage: the forgotten role of the internal conductance to CO_2 transfer. *Journal of Experimental Botany* **59**: 1475-1487.

Warren CR, Adams MA. 2006. Internal conductance does not scale with photosynthetic capacity: implications for carbon isotope discrimination and the economics of water and nitrogen use in photosynthesis. *Plant, Cell & Environment* **29**: 192-201.

Warton DI, Wright IJ, Falster DS, Westoby M. 2006. Bivariate line-fitting methods for allometry. *Biological Reviews* **81**: 259-291.

Whitehead D, Barbour MM, Griffin KL, Turnbull MH, Tissue DT. 2011. Effects of leaf age and tree size on stomatal and mesophyll limitations to photosynthesis in mountain beech (*Nothofagus solandrii* var. cliffortiodes). *Tree Physiology* **31**: 985-996.

Wright IJ, Reich PB, Westoby M, Ackerly DD, Baruch Z, Bongers F, Cavender-Bares J, Chapin T, Cornelissen JHC, Diemer M*, et al.* 2004. The worldwide leaf economics spectrum. *Nature* **428**: 821-827.

Xiang S, Reich PB, Sun S, Atkin OK. 2013. Contrasting leaf trait scaling relationships in tropical and temperate wet forest species. *Functional Ecology* **27**: 522-534.

Supporting Information

Additional Supporting Information may be found online in the Supporting Information tab for this article:

Table S1 Pearson correlations for bivariate relationships among leaf traits, when tropical and temperate species are analysed together

Table S2 Standardized major axis regression slopes and their confidence intervals for relationships comparing leaf traits of tropical and temperate species

Please note: Wiley Blackwell are not responsible for the content or functionality of any supporting information supplied by the authors. Any queries (other than missing material) should be directed to the *New Phytologist* Central Office.

Table 1 List of tropical and temperate species used in this study

Abbrev.	Family	Species	Provenance	State	Precipitation (mm)			Temperature (˚C)				Leaf chemistry		
					Annual	Driest month	Wettest month	Annual mean	Cold month minimum	Warm month maximum	Diurnal range	Leaf P area ($g\ m^{-2}$)	Leaf N area ($g\ m^{-2}$)	Chlorophyll ($g\ m^{-2}$)
PE	*Araliaceae*	*Polyscias elegans*	Mt. Molloy	QLD	1469	24	307	19.4	10.3	27.9	10.4	0.08 ± 0.01	1.69 ± 0.25	0.61 ± 0.04
FB	*Rutaceae*	*Flindersia bourjotiana*	Cape Tribulation	QLD	1860	22	402	24.1	16.2	31.3	9.0	0.08 ± 0.03	1.80 ± 0.07	0.66 ± 0.07
SS	*Myrtaceae*	*Syzygium sayeri*	Tolga	QLD	1688	32	335	20.7	10.9	29.2	10.5	0.08 ± 0.01	1.15 ± 0.13	0.39 ± 0.01
LL	*Lauracea*	*Litsea leefeana*	Cape Tribulation	QLD	1945	29	406	23.0	15.3	30.2	8.8	0.09 ± 0.01	1.20 ± 0.97	0.42 ± 0.06
DA	*Monimiaceae*	*Doryphora aromatica*	Walkamin	QLD	1501	34	303	19.6	9.2	28.6	10.9	0.09 ± 0.01	1.91 ± 0.24	0.47 ± 0.03
CA	*Fabaceae*	*Castanospermum australe*	Mareeba	QLD	2166	41	431	22.5	13.6	30.1	9.4	0.11 ± 0.02	1.50 ± 0.21	0.57 ± 0.16
										Tropical mean:		**0.09 ± 0.02** [a]	**1.58 ± 0.33** [a]	**0.52 ± 0.12** [a]
EO	*Myrtaceae*	*Eucalyptus obliqua*	Liffey	TAS	1158	48	150	9.2	0.2	20.8	10.1	0.10 ± 0.01	2.11 ± 0.15	0.57 ± 0.02
PA	*Rhamnaceae*	*Pomaderris apetala*	Liffey	TAS	1161	48	150	9.0	0.2	20.7	10.1	0.08 ± 0.02	1.54 ± 0.17	0.53 ± 0.02
EL	*Eucryphiaceae*	*Eucryphia lucida*	Strathgordon	TAS	2288	97	256	10.0	2.7	19.5	8.2	0.13 ± 0.04	1.85 ± 0.09	0.79 ± 0.05
AM	*Monimiaceae*	*Atherosperma moschatum*	Western Tiers	TAS	1181	49	153	8.8	0.0	20.4	10.0	0.11 ± 0.01	1.81 ± 0.21	0.58 ± 0.09
PC	*Phyllocladaceae*	*Phyllocladus aspleniifolius*	Cradle Mt.	TAS	1845	78	239	7.8	0.4	18.1	8.5	0.21 ± 0.04	2.05 ± 0.52	0.47 ± 0.09
										Temperate mean:		**0.13 ± 0.05** [b]	**1.88 ± 0.33** [b]	**0.57 ± 0.12** [a]

Tropical and temperate seedlings were sourced from Yuruga Native Plants Nursery, Walkamin, Queensland and Habitat Plants, Liffey, Tasmania, respectively.

Climate information, according to species provenance, was obtained from *WorldClim* (Hijmans *et al.*, 2005) using the nearest occurrence of each species in the *Atlas of Living Australia* (http://bie.ala.org.au/species/). Leaf chemistry was expressed as mean of individual species (n=4 within each species), mean values for tropical and temperate species listed in bold. Significantly different means between tropical and temperate species are indicated by different letters (P<0.05). leaf P, leaf phosphorus; leaf N, leaf nitrogen.

Species	A (µmol m^{-2} s^{-1})	g_s (mol H_2O m^{-2} s^{-1})	g_m (mol m^{-2} s^{-1} bar^{-1})	Leaf temperature (ºC)	C_a (µmol mol^{-1})	$C_i : C_a$	V_{cmax}–C_c (µmol m^{-2} s^{-1})	V_{cmax}–C_c: V_{cmax}–C_i	J_{1500}–C_c (µmol m^{-2} s^{-1})	R_{light} (µmol m^{-2} s^{-1})	R_{dark} (µmol m^{-2} s^{-1})	LMA (g m^{-2})	LDM:LFM
PE	13.1 ± 1.0	0.28 ± 0.04	0.24 ± 0.06	24.4 ± 0.2	383 ± 2	0.61 ± 0.07	64.7 ± 7.4	0.98 ± 0.04	109.9 ± 3.4	1.7 ± 0.3	1.4 ± 0.4	51 ± 8	0.32 ± 0.01
FB	10.3 ± 0.4	0.12 ± 0.02	0.22 ± 0.04	25.3 ± 0.2	387 ± 1	0.52 ± 0.03	66.6 ± 9.7	1.06 ± 0.08	109.4 ± 13.4	2.1 ± 0.3	1.2 ± 0.3	74 ± 7	0.28 ± 0.01

Table 2 Means ± standard deviation of leaf photosynthetic components and structural traits, expressed on area basis for each species

SS	8.0 ± 1.8	0.18 ± 0.05	0.15 ± 0.06	24.7 ± 0.2	389 ± 2	0.71 ± 0.05	38.2 ± 10.1	1.09 ± 0.08	61.7 ± 14.8	1.3 ± 0.3	1.0 ± 0.1	51 ± 5	0.22 ± 0.02
LL	7.8 ± 0.3	0.19 ± 0.02	0.21 ± 0.04	25.2 ± 0.4	389 ± 1	0.69 ± 0.05	35.8 ± 2.8	1.04 ± 0.05	70.3 ± 7.7	1.9 ± 0.4	1.7 ± 0.2	38 ± 4	0.23 ± 0.01
DA	6.8 ± 1.3	0.10 ± 0.02	0.16 ± 0.03	25.0 ± 0.4	390 ± 1	0.57 ± 0.07	40.2 ± 7.6	1.11 ± 0.05	73.9 ± 16.9	1.9 ± 0.2	1.3 ± 0.2	53 ± 3	0.21 ± 0.01
CA	6.0 ± 2.0	0.07 ± 0.03	0.12 ± 0.03	25.4 ± 0.5	393 ± 2	0.54 ± 0.07	39.8 ± 13.3	1.05 ± 0.07	55.8 ± 14.4	1.8 ± 0.3	1.1 ± 0.2	50 ± 3	0.33 ± 0.01
Tropical mean	**8.6 ± 2.7** [a]	**0.15 ± 0.08** [a]	**0.19 ± 0.06** [a]	**25.0 ± 0.5** [a]	**389 ± 3** [a]	**0.60 ± 0.09** [a]	**47.6 ± 15.3** [a]	**1.05 ± 0.07** [a]	**80.7 ± 24.6** [a]	**1.8 ± 0.4** [a]	**1.3 ± 0.3** [a]	**53 ± 12** [a]	**0.26 ± 0.05** [a]
EO	24.3 ± 3.6	0.62 ± 0.12	0.41 ± 0.04	24.4 ± 0.2	368 ± 5	0.67 ± 0.08	125.5 ± 26.2	1.05 ± 0.05	186.1 ± 19.1	2.7 ± 0.3	2.2 ± 0.3	58 ± 8	0.22 ± 0.02
PA	18.4 ± 2.5	0.55 ± 0.18	0.33 ± 0.06	24.3 ± 0.3	376 ± 3	0.71 ± 0.07	86.6 ± 13.3	1.09 ± 0.05	140.1 ± 19.5	2.1 ± 0.4	1.1 ± 0.2	41 ± 3	0.28 ± 0.02
EL	9.7 ± 3.9	0.12 ± 0.05	0.21 ± 0.03	25.5 ± 0.3	391 ± 2	0.46 ± 0.05	69.2 ± 25.5	1.08 ± 0.10	126.3 ± 21.2	3.1 ± 0.6	1.1 ± 0.4	79 ± 11	0.32 ± 0.02
AM	9.1 ± 1.4	0.20 ± 0.03	0.12 ± 0.04	24.7 ± 0.2	392 ± 3	0.67 ± 0.08	50.4 ± 8.9	1.17 ± 0.10	92.4 ± 14.0	2.8 ± 0.4	1.2 ± 0.4	58 ± 3	0.23 ± 0.01
PC	8.8 ± 1.3	0.13 ± 0.02	0.12 ± 0.02	24.9 ± 0.4	392 ± 2	0.57 ± 0.04	57.4 ± 10.8	1.20 ± 0.08	104.4 ± 22.3	3.0 ± 0.9	1.7 ± 0.3	97 ± 16	0.28 ± 0.04
Temperate mean	**14.3 ± 6.9** [b]	**0.33 ± 0.24** [b]	**0.23 ± 0.12** [a]	**24.7 ± 0.5** [b]	**383 ± 10** [a]	**0.62 ± 0.11**[a]	**80.3 ± 32.3** [b]	**1.12 ± 0.09** [b]	**130.1 ± 38.4** [b]	**2.7 ± 0.6** [b]	**1.5 ± 0.6** [a]	**66 ± 22** [b]	**0.26 ± 0.04** [a]

Tropical and temperate species were listed according to decreasing *A*. Tropical and temperate group means are listed in bold, calculated based on the mean of individual species (n=4 within each species). Leaf photosynthetic components were measured at 25˚C in 21% oxygen, with exception for g_m at 2% oxygen. *A*, light-saturated net photosynthesis measured at 400 µmol mol^{-1} CO_2; g_s, stomatal conductance; g_m, mesophyll conductance; C_i : C_a, ratio of intercellular CO_2 to atmospheric CO_2; V_{cmax}–C_c, maximum carboxylation velocity of Rubisco on C_c basis; V_{cmax}–C_c : V_{cmax}–C_i, the ratio of V_{cmax} on C_c basis over V_{cmax} on C_i basis; J_{1500}-C_c, rate of electron transport on C_c basis; R_{light}, respiration rate in light; R_{dark}, dark respiration rate; LMA, leaf mass per unit leaf area; LDM:LFM, leaf dry mass to leaf fresh mass ratio. Species abbreviation is provided in Table 1. Values are overall mean ± SD of leaf traits. Significantly different means between tropical and temperate species are indicated by different letters (P<0.05).

Fig. 1 Fitted curves of the response of net CO_2 assimilation rate, A (area-based) to intercellular CO_2 (C_i) at 1500 µmol quanta m^{-2} s^{-1} for (a) a tropical species *Doryphora aromatica* and (b) a temperate species *Pomaderris apetala*. Arrows point to photosynthetic rates under normal operating conditions at ambient CO_2. Circles are the measured rates of assimilation, A under 21% O_2. Dotted lines represent V_{cmax} (maximum Rubisco carboxylation capacity) predicted from Farquhar *et al.* (1980) model under 2% oxygen partial pressure, where triangles correspond to A measured in 2% O_2.

Fig. 2 Comparison of net CO_2 assimilation rate, A directly measured in 2% O_2 against A as estimated from V_{cmax} (maximum Rubisco carboxylation capacity) which was derived from fitting Farquhar *et al.* (1980) model in 2% O_2 (see dotted lines in Fig. 1). Each data point corresponded to A in 380 µmol mol^{-1} CO_2. Dashed line shows the 1 : 1 relationship.

Fig. 3 Relationships between mesophyll conductance, g_m and **(a)** net CO_2 assimilation rate, A in 400 µmol mol^{-1} CO_2 and 21% O_2, **(b)** draw-down in CO_2 in the gaseous phase and **(c)** draw-down in CO_2 in the liquid phase.

Fig. 4 (a) Relationships between V_{cmax} (maximum Rubisco carboxylation capacity) and g_m (mesophyll conductance) for tropical and temperate trees. V_{cmax} was derived from CO_2 response curves (examples shown in Fig. 1) in 21% O_2 using finite g_m (i.e. V_{cmax}–C_c). Squares corresponded to V_{cmax} of *Phyllocladus aspleniifolius* and *Litsea leefeana* depicted in (b). The dashed line was extrapolated from the points where V_{cmax}–C_c equals V_{cmax}–C_i, while the dotted line was extrapolated from *L. leefeana* illustrated in (b) and the solid line extrapolated from *P. aspleniifolius* illustrated in (b). (b) Simulations of V_{cmax} estimated with different values assumed for g_m for a temperate species *P. aspleniifolius* and a tropical species *L. leefeana* (solid lines). Squares correspond to V_{cmax} estimated using actual g_m calculated on a C_c (chloroplastic CO_2) basis and dashed lines represent V_{cmax} estimated from infinite g_m on a C_i (intercellular CO_2) basis.

Fig. 5 Comparison of maximum Rubisco carboxylation capacity, V_{cmax} estimated using finite mesophyll conductance, g_m (V_{cmax}–C_c) and assumed infinite g_m (V_{cmax}–C_i). V_{cmax} was derived from CO_2 response curves (examples shown in Fig. 1) in 21% O_2. Dashed line shows the 1 : 1 relationship. Squares corresponded to V_{cmax} of *P. aspleniifolius* and *L. leefeana* depicted in Fig. 4(b).

Fig. 6 Plots of the limitations to net CO_2 assimilation rate, A imposed by biochemistry (L_b), stomatal resistance (L_s) and mesophyll resistance (L_m) for tropical and temperate species. Error bars represent standard deviation of mean of each limitation component for each species. Tropical and temperate species was listed according to decreasing A (see Table 2). Species abbreviation is provided in Table 1.

Fig. 7 Relationships between V_{cmax} (maximum Rubisco carboxylation capacity) and J_{1500} (electron transport rate at 1500 μmol photons m^{-2} s^{-1}) estimated using finite mesophyll conductance, g_m. V_{cmax} and J_{1500} were derived from A–C_i curve in 21% O_2. Values expressed on area basis. Values of V_{cmax} and J_{1500} obtained from Xiang *et al.* (2013) using infinite g_m were plotted on the same scale. Similar patterns were observed when plotting V_{cmax} and J_{1500} on a mass basis (data not shown).

Fig. 8 Relationships between maximum Rubisco carboxylation capacity, V_{cmax} per unit leaf nitrogen, N on area basis (applying finite mesophyll conductance, g_m) and leaf mass per unit area (LMA). The line shown was inferred from the GLOPNET relationship between V_{cmax} per unit leaf N and LMA (Hikosaka, 2004; Wright *et al.*, 2004). Values of V_{cmax} per leaf N (applying infinite g_m) and LMA obtained from Xiang *et al.* (2013) were plotted on the same scale.

Fig. 9 Fitted curves of the response of net CO_2 assimilation rate, A (area-based) assuming mesophyll conductance, g_m = 0.2 mol m^{-2} s^{-1} bar^{-1} (solid lines) and assuming infinite g_m (dashed lines) to intercellular CO_2 (C_i). The grey line corresponds to the difference between C_c (chloroplastic CO_2) vs C_i based estimation of A at the same C_i, normalised to A estimated on a C_c-basis.

Figure 1

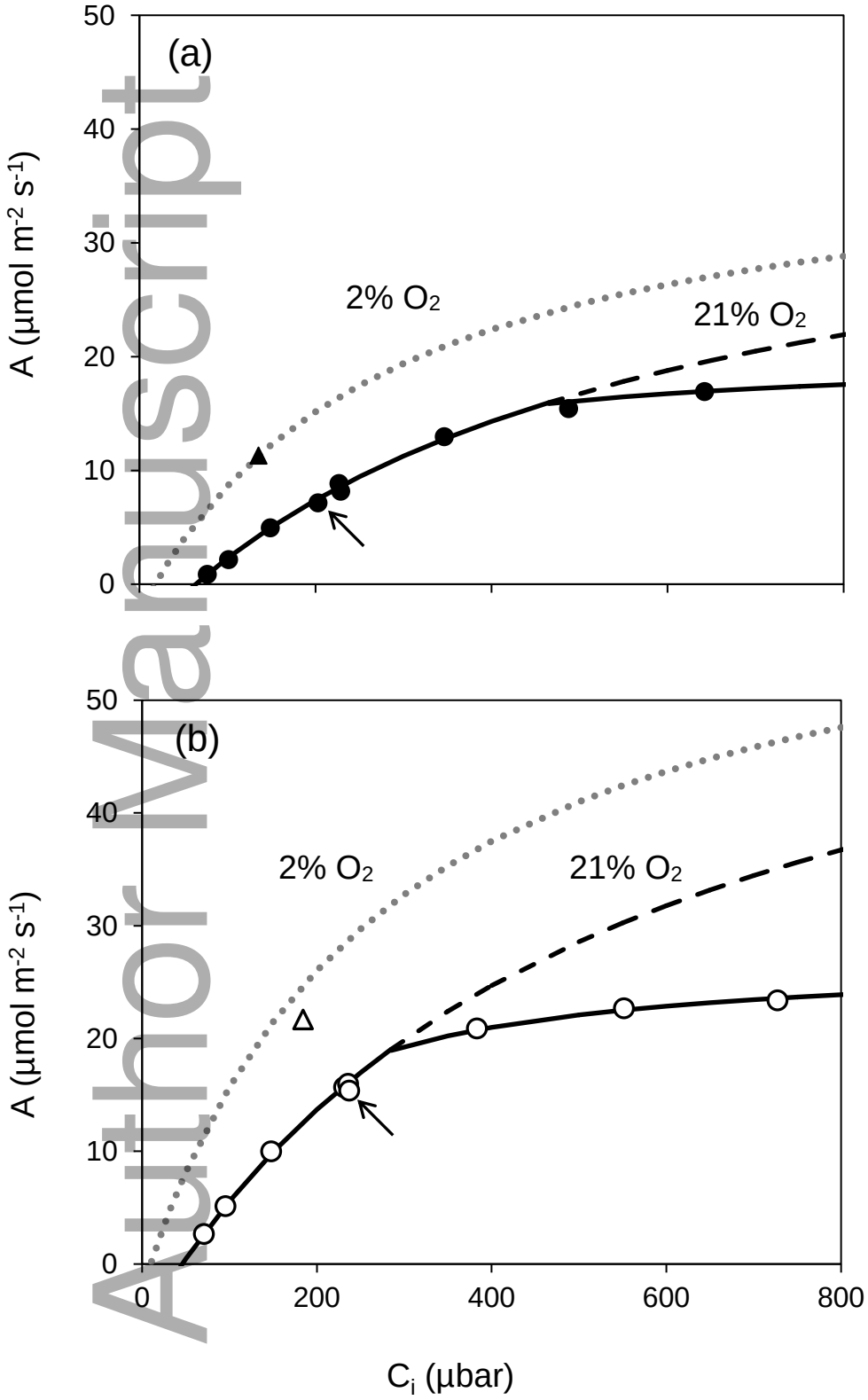

Figure 2

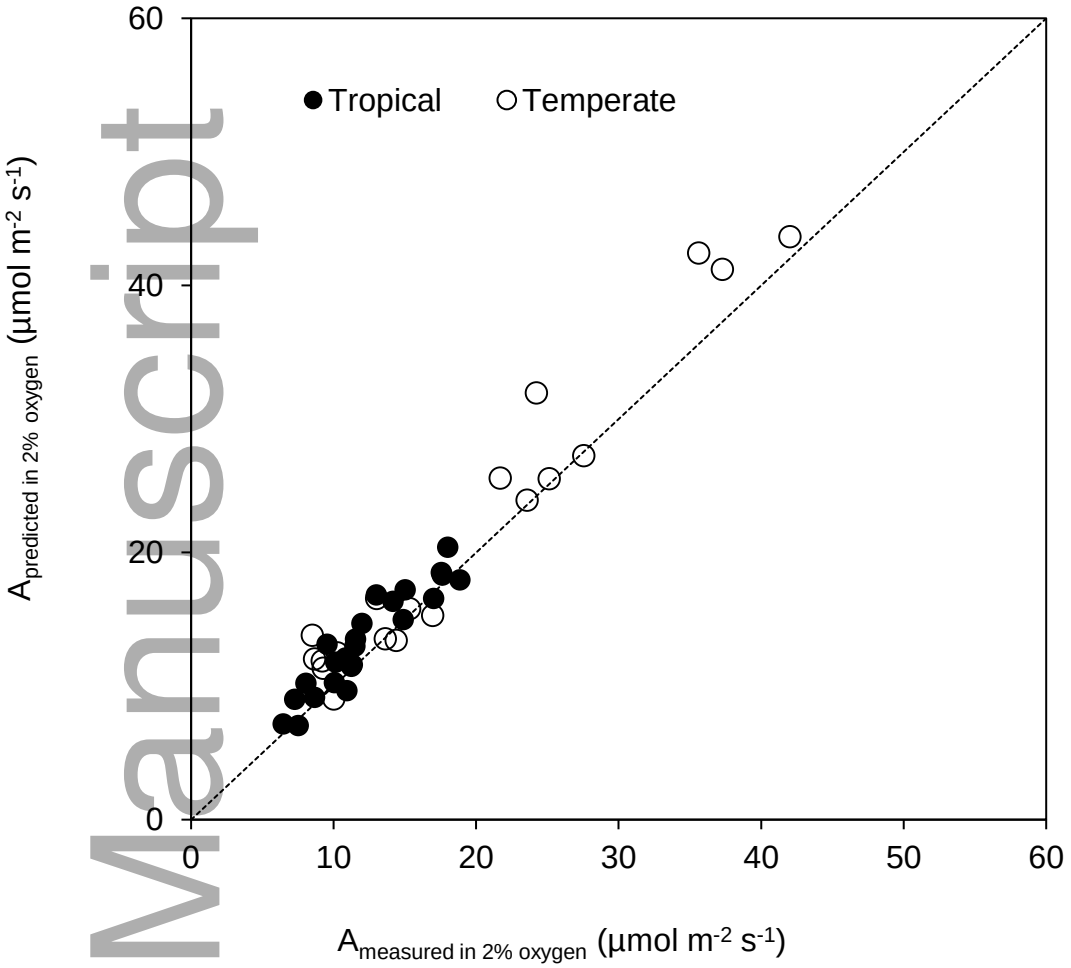

Figure 3

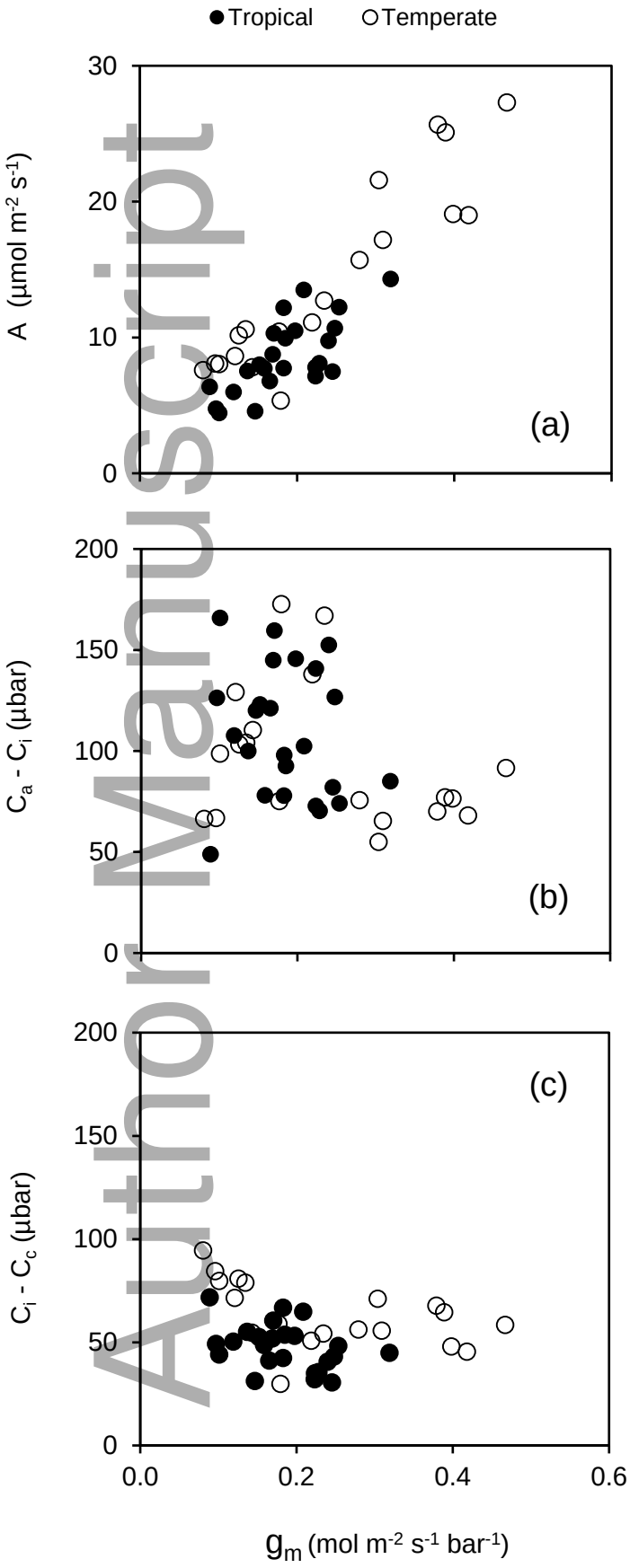

Figure 4

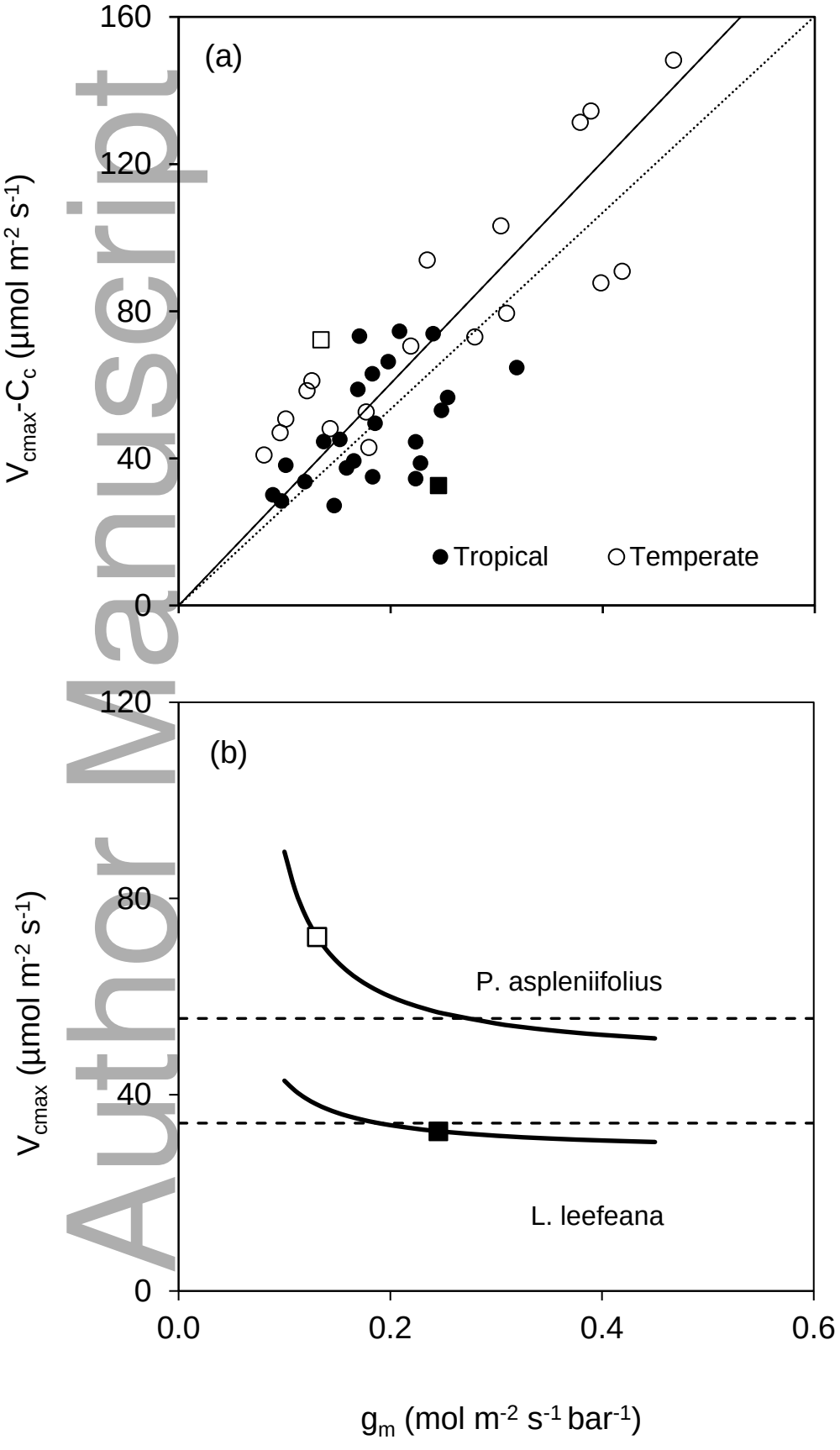

Figure 5

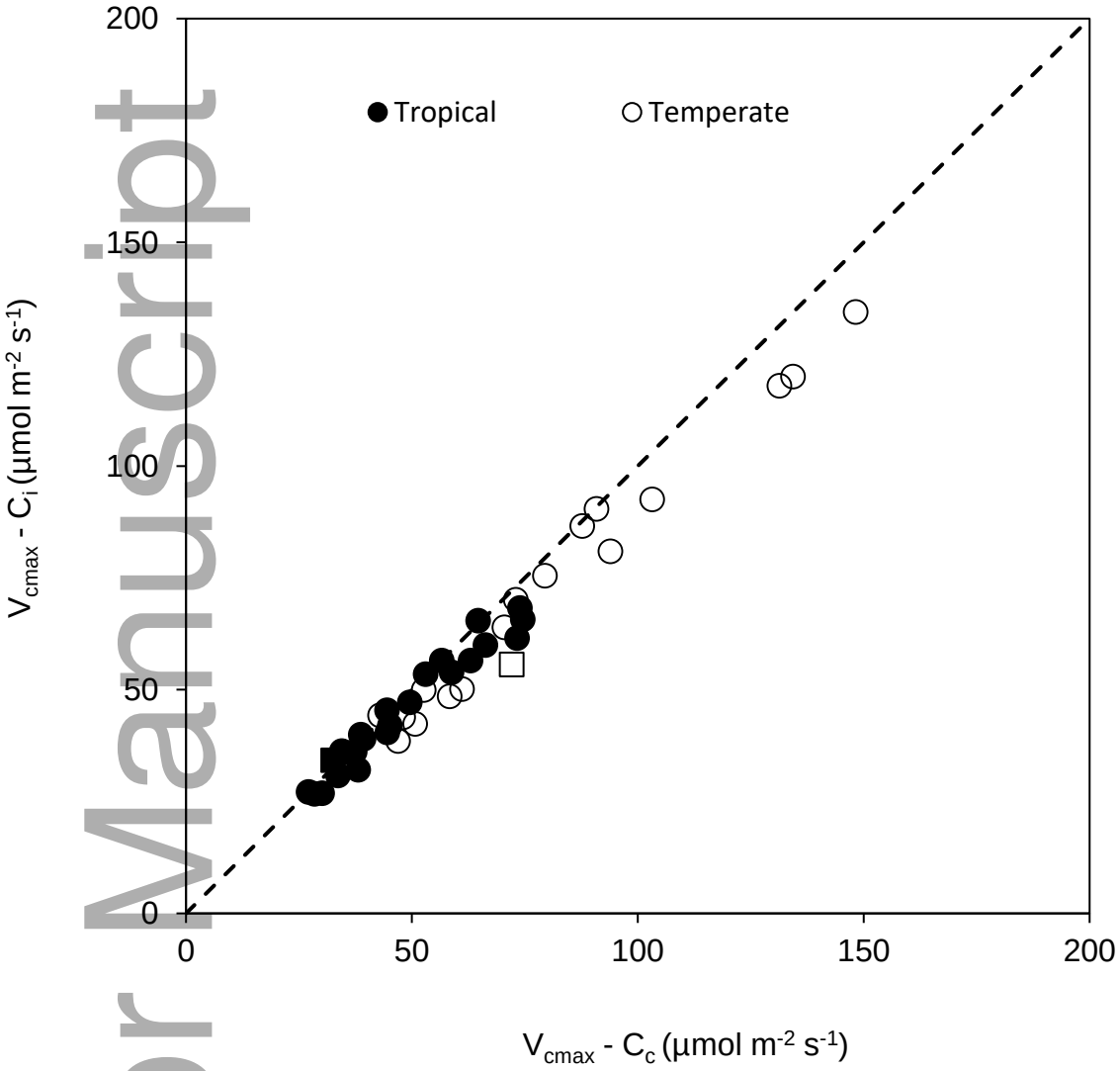

Figure 6

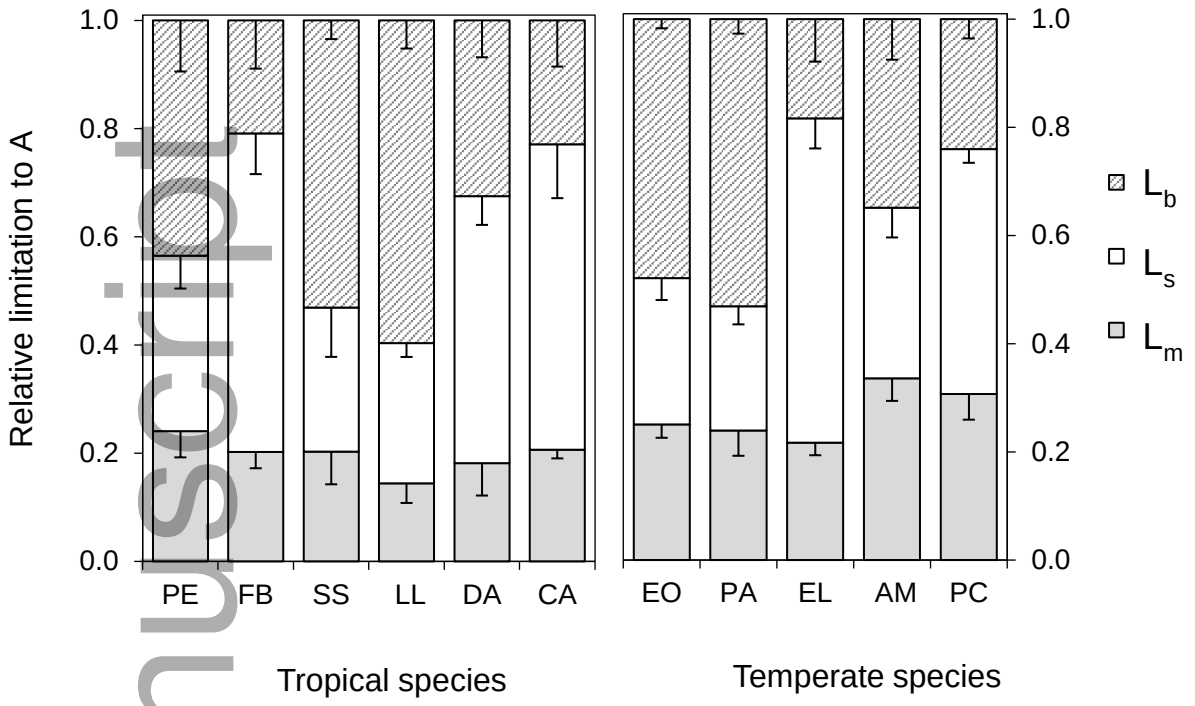

Figure 7

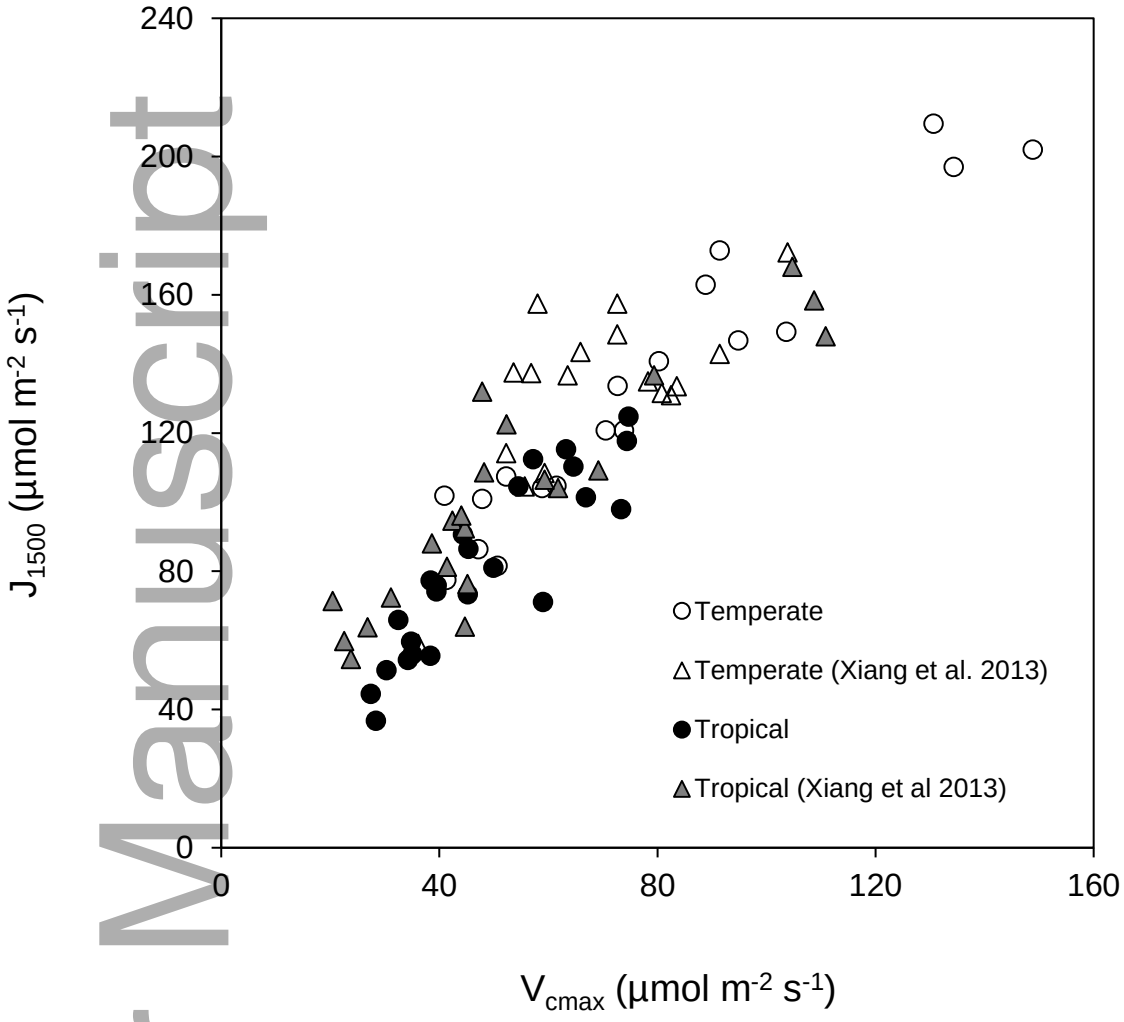

Figure 8

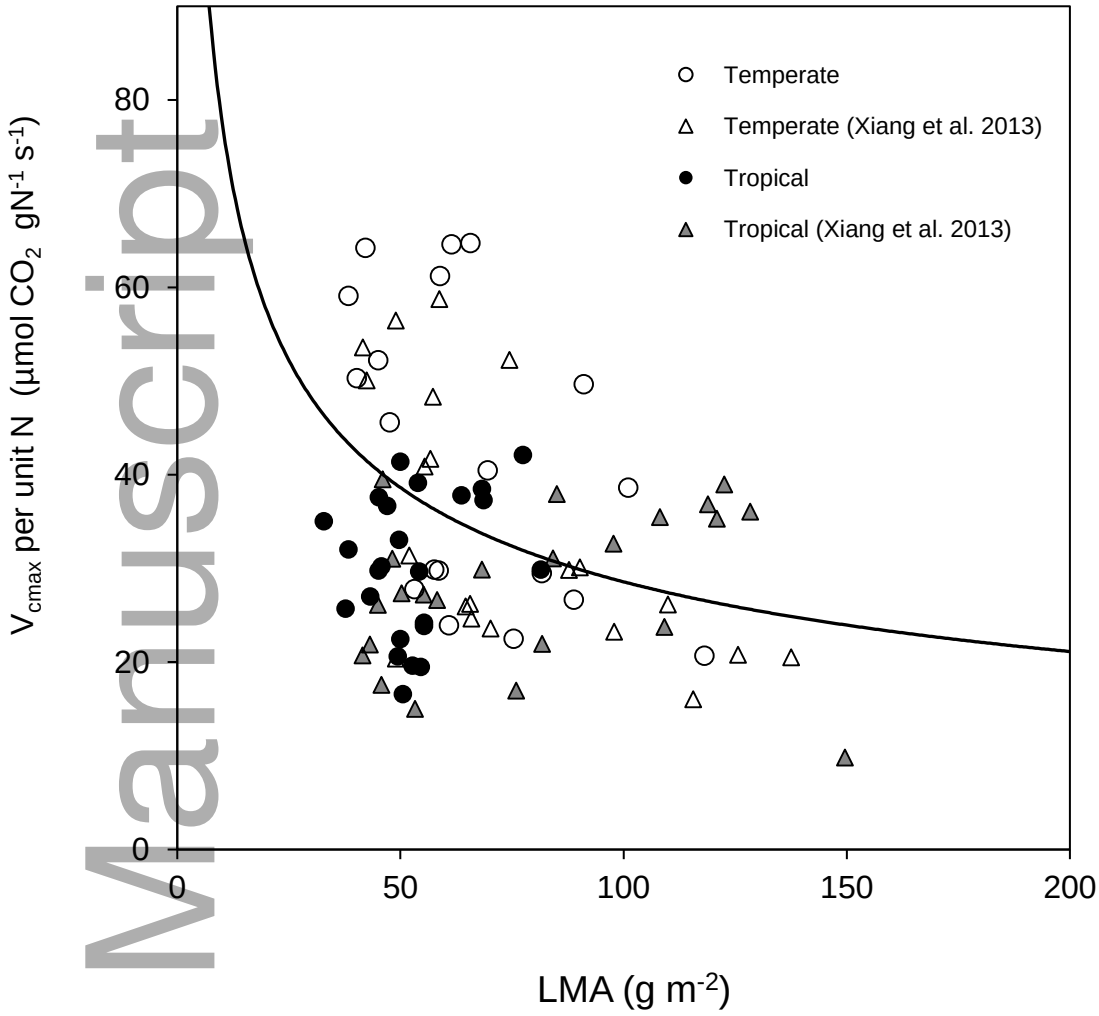

Figure 9